Titin–Actin Interaction in Mouse Myocardium: Passive Tension Modulation and Its Regulation by Calcium/S100A1

R. Yamasaki,* M. Berri,† Y. Wu,* K. Trombitás,* M. McNabb,* M. S. Z. Kellermayer,*‡ C. Witt,§ D. Labeit,§ S. Labeit,§ M. Greaser,† and H. Granzier*

*Department of Veterinary and Comparative Anatomy, Pharmacology, and Physiology, Washington State University, Pullman, Washington 99164-6520 †Muscle Biology Laboratory, University of Wisconsin, Madison, Wisconsin 53706 USA, ‡Department of Biophysics, Pécs University Medical School, Pécs H-7624, Hungary, and §Institut für Anästhesiologie und Operative Intensivmedizin, Universitätsklinikum Mannheim, Mannheim, Germany

ABSTRACT Passive tension in striated muscles derives primarily from the extension of the giant protein titin. However, several studies have suggested that, in cardiac muscle, interactions between titin and actin might also contribute to passive tension. We expressed recombinant fragments representing the subdomains of the extensible region of cardiac N2B titin (tandem-Ig segments, the N2B splice element, and the PEVK domain), and assayed them for binding to F-actin. The PEVK fragment bound F-actin, but no binding was detected for the other fragments. Comparison with a skeletal muscle PEVK fragment revealed that only the cardiac PEVK binds actin at physiological ionic strengths. The significance of PEVK–actin interaction was investigated using in vitro motility and single-myocyte mechanics. As F-actin slid relative to titin in the motility assay, a dynamic interaction between the PEVK domain and F-actin retarded filament sliding. Myocyte results suggest that a similar interaction makes a significant contribution to the passive tension. We also investigated the effect of calcium on PEVK–actin interaction. Although calcium alone had no effect, S100A1, a soluble calcium-binding protein found at high concentrations in the myocardium, inhibited PEVK–actin interaction in a calcium-dependent manner. Gel overlay analysis revealed that S100A1 bound the PEVK region in vitro in a calcium-dependent manner, and S100A1 binding was observed at several sites along titin's extensible region in situ, including the PEVK domain. In vitro motility results indicate that S100A1–PEVK interaction reduces the force that arises as F-actin slides relative to the PEVK domain, and we speculate that S100A1 may provide a mechanism to free the thin filament from titin and reduce titin-based tension before active contraction.

INTRODUCTION

Titin is a giant protein that spans the length of the half-sarcomere to form a third filament system (in addition to the thin and thick filaments) in vertebrate striated muscle (for recent reviews see Wang 1996; Labeit et al., 1997; Gregorio et al., 1999; Trinick and Tskhovrebova 1999). In the I-band, titin filaments exhibit elastic behavior upon sarcomere stretch, resulting in a force that is a primary contributor to the passive tension of cardiac muscle (Granzier and Irving 1995; Wu et al., 2000). Differential splicing of titin's primary transcript produces two classes of cardiac titin isoforms, referred to as N2B and N2BA (Freiburg et al., 2000), that differ in their expression patterns in various species. The hearts of small mammals, such as mouse and rat, express predominantly N2B titin, whereas larger mammals, including humans, co-express N2B and N2BA titins (Cazorla et al., 2000). The extensible region of N2B titin contains three subdomains: tandem Ig segments, that consist of tandemly-linked immunoglobulin (Ig)-like domains; the cardiac-specific N2B splice element, which includes a 572-residue unique sequence; and the 163-residue PEVK domain, which contains >70% (P) proline, (E) glutamic acid, (V) valine, and (K) lysine (Labeit and Kolmerer 1995). N2BA titins contain a much longer PEVK segment than N2B titins (600–800 verses 163 residues), as well as an additional tandem Ig segment and the differentially spliced N2A element (Freiburg et al., 2000). As a result, N2BA titin has a longer extensible region and higher molecular mass than N2B titin (~3.3 versus 2.97 MDa).

Immunolabeling and mechanical experiments have shown that the subsegments of titin's extensible region behave as variable-stiffness entropic springs linked in series (Linke et al., 1998a, 1998b; Trombitas et al., 1998b). As sarcomeres are stretched from their slack length, the low-stiffness tandem-Ig segments extend preferentially at short sarcomere lengths (SL), resulting in low levels of passive tension, whereas the stiffer N2B unique sequence and PEVK domain extend at intermediate to long SLs, resulting in high levels of passive tension (Helmes et al., 1999; Linke et al., 1999). The tandem Ig segments thus act as a "molecular leash" that determines the SL range in which titin's primary force-generating elements, the N2B unique sequence and the PEVK domain, operate.

Recent studies have suggested that passive tension in cardiac muscle may not be solely determined by titin's intrinsic elasticity, but may also include contributions from titin–actin interaction (Granzier et al., 1997; Stuyvers et al., 1997a,b, 1998, 2000). This suggestion is supported by titin's close proximity to the thin filament in the I-band, and by previous reports of binding between titin and actin, both in vitro and in situ (Kimura et al., 1984; Funatsu et al., 1993;

Received for publication 30 April 2001 and in final form 27 June 2001.

Address reprint requests to H. Granzier, Dept. of Veterinary and Comparative Anatomy, Pharmacology, and Physiology, Washington State University, Pullman, Washington 99164-6520. Tel.: 509-335-3390; Fax: 509-335-4650; E-mail: granzier@wsunix.wsu.edu.

0006-3495/01/10/2297/17 $2.00

Jin 1995; Kellermayer and Granzier 1996a,b; Linke et al., 1997; Trombitas and Granzier 1997). Of particular interest are potential interactions involving titin's extensible region, because these would be most likely to influence the passive mechanical properties of cardiac muscle.

To study titin–actin interaction, we expressed recombinant fragments representing the subdomains comprising titin's extensible region, and surveyed them for binding to F-actin. Because animal models that express predominantly N2B titin (mouse and rat) have been extensively studied and are readily available, we focused our work on the N2B isoform. Our results reveal that only the PEVK region of N2B titin binds F-actin. We also studied a second PEVK fragment expressed in skeletal muscle titins, and found that, although it can also bind F-actin, the binding is weaker than that observed with the N2B PEVK, and does not occur at physiological ionic strengths (IS). These results suggest that, within titin's extensible segment, the cardiac N2B PEVK domain may be unique in its ability to bind F-actin.

The physiological significance of PEVK–actin interaction was investigated using an in vitro motility assay technique and mechanical experiments with single mouse cardiac myocytes. Our findings suggest that, as the thin filament slides relative to titin during passive muscle stretch, a dynamic interaction between the PEVK domain and F-actin results in a force that opposes filament sliding and enhances passive tension. We also explored potential calcium effects on PEVK–actin interaction. Although calcium alone exerted no effect, we found that S100A1, a member of the S100 family of EF-hand calcium binding proteins, regulates PEVK–actin interaction in a calcium-dependent manner. The regulation of PEVK–actin interaction by calcium/S100A1 may provide a mechanism to free the thin filament from titin before active contraction, and to reduce titin-based force during systole.

MATERIALS AND METHODS

Recombinant titin fragments

Titin cDNA fragments (Fig. 1*A*) were amplified by polymerase chain reaction (PCR) using primer pairs derived from human cardiac N2B titin (EMBL data library accession X90568) and human soleus skeletal muscle titin (accession X90569). Fragments were cloned into modified pET vectors, expressed in BL21[DE3]pLysS cells, and purified from the soluble fraction on Ni-NTA columns with a His-Bind purification kit (Novagen, Madison, WI). Fragment boundaries from the human cardiac N2B peptide sequence corresponded to: I91–I98 (residues 5237–5959), I91–I94 (5237–5591), I27-PEVK-I84 (residues 4337–4713), and uN2B (residues 3671–4242). The skeletal muscle PEVK fragment (sPEVK) included residues 5898–6377 of the human soleus peptide sequence. All fragments were purified under native conditions, except I27-PEVK-I84, which degraded and aggregated under these conditions. I27-PEVK-I84 was thus column-purified in the presence of 6M GuCl and 10 mM glutathione, and refolded while bound to the column via a gradient-to-native binding buffer ((mM) 5 imidazole, 500 NaCl, 20 tris-HCl, pH 7.9) as described previously (Zahn et al., 1997). This treatment reduced aggregation and significantly increased the purity of the preparation (Fig. 1 *B*). Samples were then quick frozen in liquid nitrogen and stored at −80°C. Upon thawing, I27-PEVK-I84 sometimes contained a small fraction of aggregate species. Therefore, samples were thawed immediately before all experiments, and residual aggregates were removed via centrifugation for 30 min in a Beckman Airfuge at 30 psi. The samples were then stored on ice and used within 1 h. Circular dichroism spectroscopic measurements were performed to ensure that the Ig-like domains flanking the PEVK domain (I27 and I84) were properly folded during purification (Fig. 1*C*). Our results are similar to those obtained previously for I91 (Politou et al., 1995; here referred to as I27), with a maximum at ~200 nm, and a minimum at ~212 nm. The β-sheet content of our fragment was estimated at ~57% using the software program CD ESTIMA (based on Chang et al., 1978). This value is consistent with previous estimates for a titin Ig-like domain (Politou et al., 1994). All fragments were dialyzed into (mM) 100 KCl, 25 imidazole (pH 7.4) and 1 DTT before use, and protein concentrations were determined via the Bradford method (Bradford, 1976). Theoretical isoelectric points were calculated with the MW/PI calculator at http://www.expasy.ch.

Proteins

Actin, myosin, and heavy meromyosin (HMM) were purified according to the methods of Pardee and Spudich (1982), Margossian and Lowey (1982), and Kron et al. (1991), respectively. The purity of protein preparations was monitored by SDS-gel electrophoresis on 12% gels, and concentrations were determined via absorbance at 280 nm using molar extinction coefficients of 1.1 cm^{-1}, 0.53 cm^{-1}, and 0.6 cm^{-1} for actin, myosin, and HMM, respectively. F-actin was fluorescently labeled with a 1.5X molar excess of tetramethyl-rhodamine-isothiocyanate-conjugated phalloidin (Molecular Probes, Eugene, OR) and S100A1 was purchased from Calbiochem (La Jolla, CA; catalog #559287).

Co-sedimentation assay

F-actin was incubated at room temperature for 20 min with recombinant titin fragments in co-sedimentation buffer ((mM) 100 KCl, 25 Imidazole-HCl (pH 7.4), 1.5 $MgCl_2$, 1 ATP, 1 DTT, and either 1 EGTA or 0.1 $CaCl_2$) in a total volume of 50 μl. The mixtures were then sedimented in a Beckman Airfuge at 28 psi for 30 min. After removing the supernatants, pellets were washed with 100 μl co-sedimentation buffer, and allowed to stand in an additional 50 μl co-sedimentation buffer. The pellets and supernatants were solubilized at 90°C for 3 min with 25 μl of 3X solubilization buffer (Laemmli 1970), electrophoresed on 12% SDS gels, and stained with Coomassie Blue. The gels were then scanned with an Epson 800 optical scanner, and densitometry was performed using the One-D-Scan software program (v.1.31, Scanalytics Corporation). For Kd determinations, data were fit with a one-site saturable binding function (Y = Bmax*X/Kd + X).

Fluorescent surface-binding assay

The visual binding assay was carried out essentially according to Kellermayer and Granzier (1996a). Experiments were performed in a flow-through microchamber with an internal volume of ~10 μl, whose surface was coated with 1% nitrocellulose (Ernest Fullam, Latham, NY). Fluorescent F-actin was sheared three times with a 27-gauge needle before use to give a uniform length distribution (estimated mean length ~1–2 μm). Solutions were added to the assay chamber in the following order: Experiments in Fig. 3: (μl) 25 PEVK, 100 1-mg/ml BSA (blocking), 100 wash (twice), 100 fluorescent F-actin, and 100 wash, with 1-min incubation periods following each step. All components were in buffer A ((mM) 25 imidazole-HCl (pH 7.4), 1.5 $MgCl_2$ (free $[Mg^{2+}]$ ~1.5 mM), 1 DTT, and KCl to achieve specified IS). Buffer A in PEVK and blocking steps had an IS of 180 mM. For steps following blocking, buffer A contained 1 mM

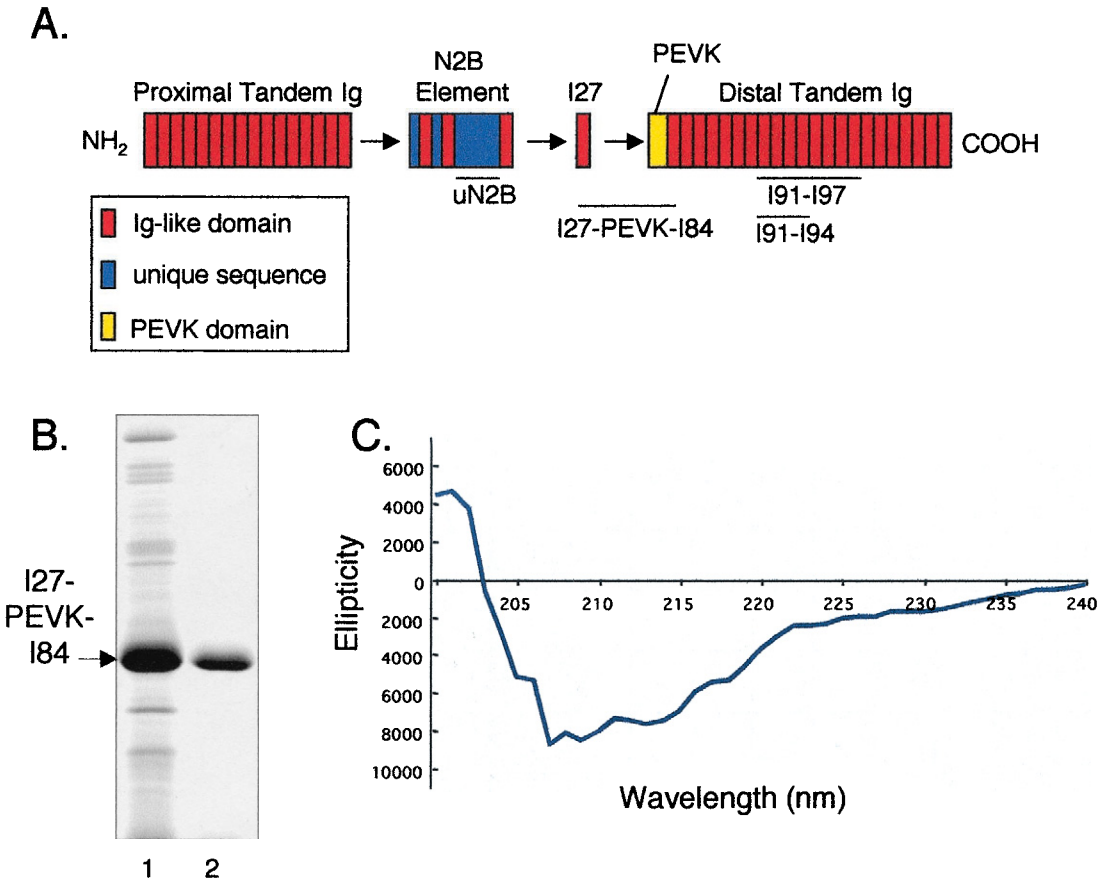

FIGURE 1 Recombinant titin fragments. (*A*) Domain organization of the extensible I-band segment of human cardiac titin (N2B isoform; accession X90568), with the compositions of fragments denoted by lines under their corresponding locations in the sequence. (Domain numbering is according to Freiburg et al.; 2000. (*B*) Coomassie stained 12% SDS-gel of I27-PEVK-I84. *Lane 1* was purified under standard (native) conditions, and *lane 2* was column-purified under denaturing conditions and refolded while bound to the column. The denaturing/refolding procedure significantly enhanced the purity of the preparation. The identity of the I27-PEVK-I84 band was confirmed via western blots with the 9D10 anti-PEVK antibody (Wang and Greaser; 1985; Trombitas et al., 1998a; Greaser et al., 2000). (*C*) CD spectrum of denatured/refolded I27-PEVK-I84. The spectrum is similar to that determined previously for the titin Ig-like domain I91 (see Methods), and indicates that I27 and I84 have likely assumed their proper β-barrel structures.

EGTA and had variable IS. Experiments in Fig. 8: (μl) 25 PEVK, 100 1-mg/ml BSA (blocking), 100 wash (twice), 100 S100A1. (Wash in control experiments), 100 1-mg/ml BSA, 100 wash, 100 fluorescent F-actin, and 100 wash, with 1-min incubation periods following each step. The IS of buffer A was 180 mM, and, for steps following blocking, buffer A contained 0.1 mM $CaCl_2$ or 1 mM EGTA (see Fig. 8 *A*), or 1 mM EGTA and $CaCl_2$ to achieve specified pCa (see Fig. 8 *B*. Ionic strength and pCa ($-\log[Ca^{2+}]$) were calculated using the software program of Fabiato (1988). Experiments were carried out at room temperature. Fluorescent actin filaments were visualized via epifluorescence microscopy and images were captured and recorded as described previously (Kellermayer and Granzier 1996a). Twenty randomly selected microscopic fields of view (FOV) were recorded for each experiment, and the number of bound actin filaments per FOV was measured using a user-developed program for Scion Image image analysis software (v. 1.6; based on NIH Image, National Institutes of Health, Bethesda, MD).

In vitro motility

In vitro motility experiments were carried out essentially according to Kron et al. (1991), using the setup described by Kellermayer and Granzier (1996a). The temperature was controlled at 27°C by a jacketed objective thermostat. A flow-through chamber similar to that described for the fluorescent surface-binding assay was used, with double-thickness spacers and an internal volume of ~20 μl. Solutions were added to the assay chamber in the following order: Experiments in Fig. 4: (μl) 50 HMM or HMM + PEVK (mixed immediately before use), 100 0.5-mg/ml BSA (blocking), 100 wash (twice), 100 fluorescent F-actin, 100 0.5-mg/ml BSA, 100 motility buffer (supplemented with an enzyme cocktail to reduce photo-bleaching (Kron et al., 1991), ATP to give a pMg-ATP of 3.0, $MgCl_2$ to give free [Mg] of 1.5 mM, and 0.7% w/v methylcellulose). All components were in buffer B ((mM) 25 Imidazole-HCl (pH 7.4), 1.5 $MgCl_2$, 1 EGTA, 1 DTT, and K-propionate to give IS of 140). Experiments in Fig. 9: (μl) 50 HMM or HMM/PEVK, 100 0.5-mg/ml BSA (blocking), 100 wash (twice), 100 3-μM S100A1 (wash in control), 100 0.5-mg/ml BSA, 100 wash, 100 fluorescent F-actin, 100 0.5-mg/ml BSA, 100 motility buffer, as described above. All components were in buffer B with either 1 mM EGTA or 0.1 mM $CaCl_2$, except the PEVK and blocking steps in which EGTA/calcium was omitted. Each step in the motility experiments was followed by a 1-min incubation at room temperature. Solution compositions were calculated according to Fabiato (1988).

Images of moving filaments were visualized, recorded, and digitized as described by Kellermayer and Granzier (1996a). Filament velocities were measured from digitized movies (30 frames; 10 frames/s) using user-

developed programs for the Scion Image software program. Velocities were calculated by measuring the centroid positions of selected filaments as a function of time. Completely or partially immobile filaments (those with any part of the filament immobilized on the substrate for greater than a 5-frame (0.5-s) interval) and those undergoing nontranslational movement (e.g., spiraling as described by Gordon et al., 1997) were omitted from analysis. Velocities were determined for 75 filaments in ~5–10 FOV for each experiment. A 10-μm optical grating (VWR Scientific, Seattle WA) was used for spatial calibration.

Capillary binding assay

The experimental protocol was similar to that described previously (Li et al., 1995; Kellermayer and Granzier 1996a). Glass capillaries with an internal volume of 100 μl (VWR Scientific) were coated with 1% nitrocellulose (Ernest Fullam, Latham, NY), dried, and incubated with the following solutions: 0.2 mg/ml PEVK (omitted in negative control), blocking solution (5% w/v BSA, 1% w/v gelatin), 0.5% w/v BSA (twice), 0.2 mg/ml HMM, and wash (5×). All components were in 180 mM buffer A. Bound proteins were then solubilized by repeatedly rinsing capillaries with 1X solubilization buffer (Laemmli 1970) at 90°C, electrophoresed on a 12% SDS-gel, and silver stained according to the method of Granzier and Wang (1993).

Myocyte mechanics

Cardiac myocytes were isolated from mouse left ventricle according to the method of Wolska and Solaro (1996), and skinned as described previously (Granzier and Irving 1995). Passive tension–SL curves were obtained as detailed in Helmes et al. (1999). Experiments were performed in an open chamber with an internal volume of ~300 μl, and passive tension was measured in relaxing solution ((mM) 25 imidazole-HCl (pH 7.4), 100 KCl, 7.5 Mg-acetate (free magnesium = 3.55 mM), 5 EGTA, 3.3 ATP, 12 creatine phosphate, 1 DTT, 0.04 leupeptin, and 0.01 E-64). Cells were activated with a pCa 4.5 (pCa adjusted with $CaCO_3$) activating solution before passive tension measurements to verify cell quality. Control passive tension–SL relations were measured by applying a slow-ramp stretch–release (0.1 lengths/s), and cells were then incubated in ~2.8 μM I27-PEVK-I84 (achieved via 2 half-volume changes of the chamber solution with 3.75 μM I27-PEVK-I84 in relaxing solution, with 10- and 30-min incubation periods after each change, respectively). Low-amplitude stretch–releases (SL ~ 1.9–2.2 μm) were imposed every 5 min during PEVK incubation to facilitate diffusion of the fragment. Passive tension–SL curves were then obtained in the presence of I27-PEVK-I84, followed by washout of the fragment via continuous perfusion for 20 min, and measurement of passive-tension-SL curves after washout. Experiments were conducted at room temperature.

Gel overlay

Fragment I27-PEVK-I84 was electrophoresed (~1 μg/lane) on 12% SDS-gels and transferred to PVDF membrane with constant current. To facilitate transfer of the basic fragment (pI ~ 9.7), blotting buffers were pH 11.7. After transfer, membrane strips were washed extensively in distilled H_2O, followed by buffer C ((mM) 25 imidazole-HCl (pH 7.4), 4 $MgCl_2$, 1 DTT, either 1 EGTA or 0.1 $CaCl_2$, 0.05% Tween-20 and KCl to give IS of 140). The strips were then blocked with 0.5% w/v BSA and 0.2% w/v gelatin in buffer C, washed with buffer C, and incubated for 30 min at room temperature with biotinylated S100 (S100A1 was biotinylated with a biotin-X-NHS kit (Molecular Probes) according to the suppliers instructions). After extensive washing with buffer C, the strips were incubated for 30 min with an avidin-conjugated alkaline phosphatase (Vector laboratories, Burlingame, CA), washed with buffer C, and developed with Sigmafast BCIP/NBT substrate (Sigma, St. Louis, MO). Biotinylated S100 was excluded from negative control experiments. Scanning and densitometry was performed as described for co-sedimentation assays.

Immunolabeling and electron microscopy

Left ventricular wall muscle was dissected from mouse hearts in HEPES buffer ((mM) 10 HEPES (pH 7.4), 133.5 NaCl, 4 KCl, 1.2 $NaHPO_4$, 1.2 $MgSO_4$, and 11 D-glucose), and skinned overnight in skinning buffer (relaxing solution with 1% triton X-100). Muscle strips were dissected in skinning buffer, stretched to ~10, 20, or 30% of their slack length, and pinned to a Sylgard (Dow Corning Corporation, Midland, MI) surface on the bottom of ~100 μl wells. The wells were washed 20×, for 3 min each with rigor buffer (RB) ((mM) 40 imidazole-HCl (pH 7.0), 10 EGTA, 0.5 Mg-acetate, 5 Na-azide, 140 K-propionate, 0.4 leupeptin, 0.1 E-64, 0.5 PMSF, and 1 DTT) containing 2% triton X-100. After the rigor washes, plates were separated into 2 groups that were treated in all subsequent steps with RB, with (pCa 4.5) or without (pCa 9) calcium. Wells were then washed an additional 5× in RB for 3 min each, followed by blocking with 0.5% (w/v) BSA in RB for 30 min. After a 10-min wash with RB, the strips were incubated with 7.5 μM S100A1 for 30 min (RB in controls), washed for 3 min in RB, and lightly fixed with 0.3% paraformaldehyde in RB for 20 min. Immunodetection and electron microscopy were performed as described previously (Granzier et al., 1996) using a primary antibody to the S100 α-subunit (Sigma, catalog# S-2407). Epitope distances with respect to the Z-line were measured from scanned negatives of electron micrographs using an user-developed program for Scion Image software.

RESULTS

The cardiac titin PEVK domain binds F-actin

Recombinant fragments representing the subdomains of cardiac N2B titin's elastic segment (tandem Ig segments, the PEVK domain, and the N2B splice element) were expressed in *Escherichia coli* and purified from the soluble protein fractions. The fragments (Fig. 1 *A*) included: the 572-residue unique sequence in the cardiac-specific N2B element (uN2B); four and eight Ig-like domain fragments from the distal tandem Ig segment (I91-I94 and I91-I97); and the N2B PEVK domain along with its flanking Ig-like domains, I27 and I84 (I27-PEVK-I84). To investigate potential interactions between F-actin and titin's extensible region, co-sedimentation assays were performed. In the absence of F-actin, each of the fragments was found predominantly in the supernatant, whereas, in the presence of F-actin, only the PEVK fragment was detected in the pellet (Fig. 2*A*). The absence of F-actin binding by I91-I97 indicates that the binding exhibited by I27-PEVK-I84 is unlikely to be mediated by the flanking Ig-like domains, and requires the PEVK domain. The co-sedimentation results suggest that the I27-PEVK-I84 region is unique within cardiac titin's extensible segment in its ability to bind F-actin. However, there are subdomains within the extensible segment that are not represented by our recombinant fragments, and for which actin binding cannot be excluded. These include two of titin's Ig-like domains in

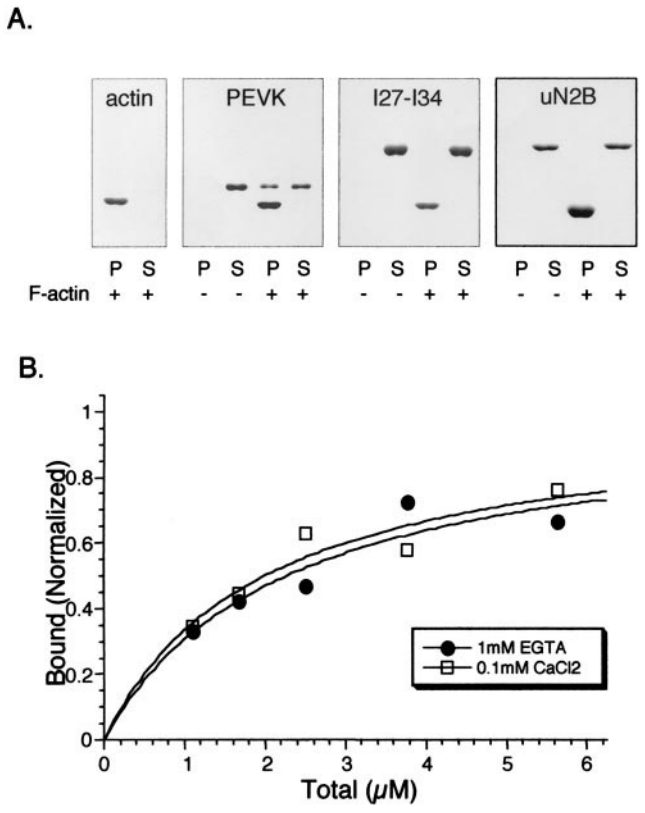

FIGURE 2 Survey of actin-binding propensities along titin's extensible region. (*A*) Co-sedimentation assay. Fragments (2.75 μM) representing the subsegments comprising titin's extensible region (tandem-Igs (I91–I98), N2B element (uN2B), and the PEVK domain (I27-PEVK-I84)) were assayed for binding to F-actin (5 μM). In control experiments, the fragments were found in the supernatant, whereas, in the presence of F-actin, only I27-PEVK-I84 was detected in the pellet. (*B*) Kd determination for F-actin binding to I27-PEVK-I84. 2.5 μM F-actin was incubated with varying concentrations of I27-PEVK-I84 (5.6–1.1 μM) in the presence (0.1 mm $CaCl_2$; squares) or absence (1 mM EGTA, *circles*) of calcium. Densitometric analysis yielded Kd values of 2.27 ± 1.1 and 2.0 ± 0.8 μM in the presence and absence of calcium, respectively.

the proximal tandem Ig segment (I14 and I15) that contain ~10–15-residue C-terminal extensions (Witt et al., 1998), and two additional unique sequence insertions (21 and 48 residues in length) in the N2B element (Fig. 1 *A*). Future work will be required to determine whether these regions can also bind F-actin.

The affinity of I27-PEVK-I84–F-actin interaction was estimated via co-sedimentation (Fig. 2 *B*) with varying concentrations of the PEVK fragment (1–5.5 μM) and a fixed amount of F-actin (2.5 μM). Because there is a previous report of a calcium-dependent interaction between thin filaments and purified full-length titin (Kellermayer and Granzier, 1996a), the experiments were conducted in both the presence (0.1 mM $CaCl_2$) and absence (1 mM EGTA) of calcium. The data gave Kd values of 2.27 ± 1.1 and 2.08 ± 0.8 μM in the presence and absence of calcium, respectively. These values indicate that titin's PEVK region binds F-actin with moderate affinity, in a manner that is unaffected by calcium. The Kd values are also very similar to those recently reported for F-actin binding to a fetal skeletal muscle PEVK fragment (Kd ~ 1–5 μM) using an independent method (Gutierrez-Cruz et al., 2000). The absence of a calcium effect on PEVK–actin interaction suggests that the calcium-dependent interaction observed by Kellermayer and Granzier (1996a) was mediated by titin domains outside of the regions examined in the present study.

PEVK–actin interaction occurs at physiological ionic strengths

Interactions involving F-actin are often IS dependent, and we thus performed additional binding studies to assess the effect of IS on PEVK–actin interaction. For these studies, a visual fluorescence assay was used similar to that described previously by Kellermayer and Granzier (1996a). This approach has the advantage of requiring small quantities of proteins, allowing F-actin interactions to be assayed under a wide variety of conditions. Furthermore, the assay has only one freely diffuseable binding partner. This arrangement may be more relevant to conditions in the sarcomere, where the thin filament is anchored in the Z-line.

Figure 3 *A* (*left*) shows a microscopic field of view with fluorescent F-actin bound to a PEVK-coated surface. The panel on the right shows a field with an absence of binding to a BSA-coated surface (negative control). I91–I97 and uN2B-coated surfaces displayed a similar absence of F-actin binding (not shown). These results agree with our co-sedimentation results, and indicate that, within titin's extensible segment, the PEVK region is unique in its ability to bind F-actin. Figure 3 *B* (*squares*) shows the relative degree of binding between F-actin and the I27-PEVK-I84 as a function of IS . The binding is unaffected by increased IS to a value of ~170 mM. At values greater than 170 mM, the number of bound filaments decreased with increasing IS. Half-maximal binding was observed at an IS of ~190 mM. The interaction between F-actin and the PEVK fragment is thus sensitive to the IS, while being significant within the physiological range in striated muscle (170–200 mM; Maughan and Godt 1989).

Because of a recent report of F-actin binding to a fetal skeletal muscle PEVK fragment (Gutierrez-Cruz et al., 2000), we also expressed an ~500-residue skeletal PEVK fragment (sPEVK) and tested whether it bound F-actin in the visual binding assay. No binding was observed when the sPEVK fragment was added to the assay chamber at the same concentration as I27-PEVK-I84. Upon introducing successively higher concentrations of sPEVK, significant binding was observed at intermediate (110 mM) IS with an sPEVK concentration approximately 10-fold higher than that used for I27-PEVK-I84.

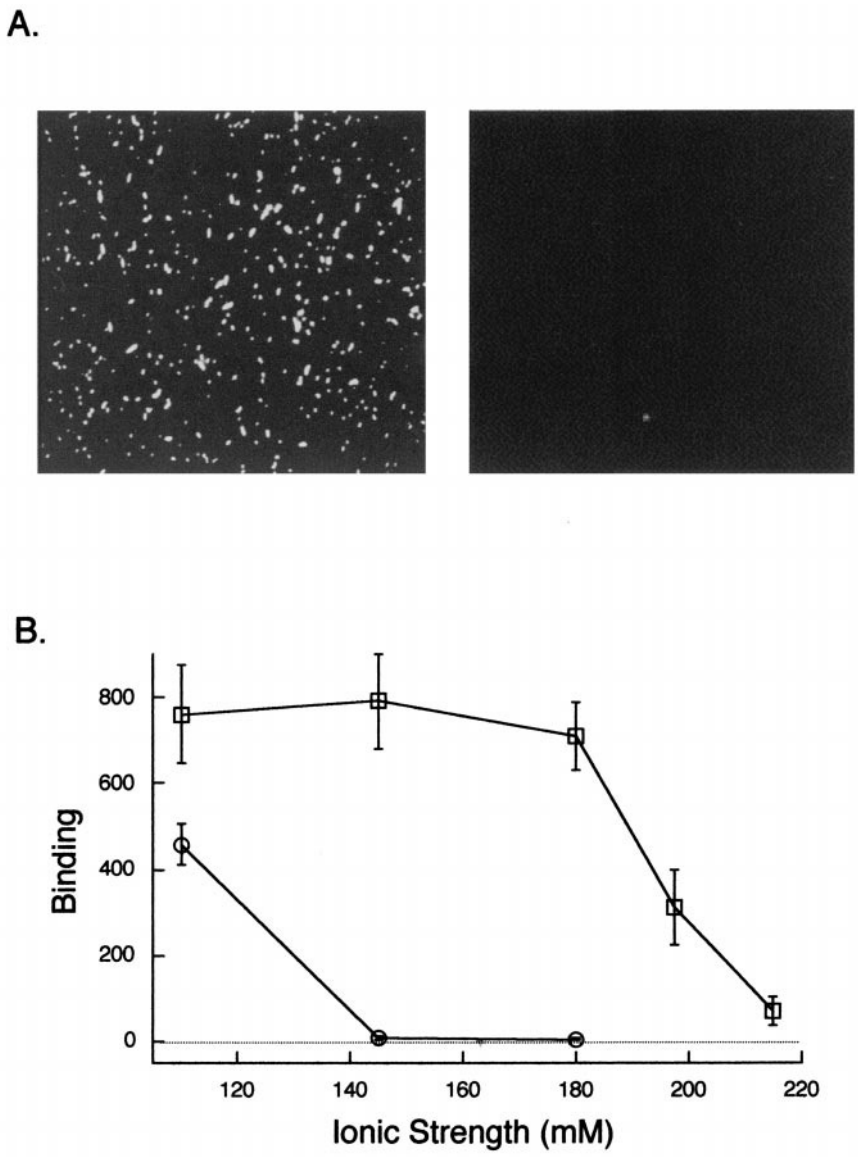

FIGURE 3 Fluorescent surface-binding assay. (*A*) *Left:* Microscopic image showing fluorescently labeled F-actin bound to a surface coated with I27-PEVK-I84. *Right:* F-actin did not bind to a BSA-coated surface. (*B*) Binding as a function of IS. The mean number of actin filaments bound per microscopic FOV to 0.3 μM I27-PEVK-I84 (*squares*) and to 2.5 μM sPEVK, an ~500-residue skeletal muscle PEVK fragment (*circles*), as a function of IS. I27-PEVK-I84 binds F-actin at physiological (~170–200) IS, whereas sPEVK does not. $N = 5$ experiments at each IS, with bound filaments counted for 20 FOV in each experiment. Error bars are $\pm$ SD.

The observed binding exhibited an enhanced IS sensitivity, however, and no binding could be detected at IS values greater than 145 (Fig. 3 *B*, *circles*). These findings indicate that, although the sPEVK fragment can interact with F-actin, it binds with a much weaker affinity and increased IS sensitivity compared to the cardiac PEVK. Gutierrez-Cruz et al. (2000) found similar properties with a fetal skeletal muscle PEVK fragment, which bound F-actin at intermediate, but not physiological levels of IS. The results of the binding studies conducted with skeletal PEVK fragments therefore suggest that only the cardiac N2B PEVK domain can bind F-actin under physiological IS conditions.

PEVK–actin interaction inhibits in vitro motility

The elastic behavior of the cardiac PEVK domain in vivo requires that an interaction between it and the thin filament be dynamic in nature. An in vitro motility assay technique was therefore used to investigate the physiological significance of PEVK–actin interaction under dynamic conditions. The velocities of actin filaments sliding over a surface

coated with either HMM or a mixture of HMM and the PEVK fragment were measured in the presence of 1 mM EGTA. This protocol simulates the arrangement in passive muscle, where the thin filaments slide relative to titin as sarcomeres are stretched.

The PEVK fragment inhibited sliding velocities in a concentration-dependent manner (Fig. 4, *circles*), with an ~0.5 μM concentration of the fragment resulting in a ~70% decrease in velocity relative to the control (HMM only). To test for nonspecific effects, a fragment containing the Ig-like domains I91–I94 from titin's proximal tandem Ig segment was used in parallel experiments. The four-domain I91–I94 fragment, which has a similar molecular weight to the PEVK fragment, had no significant effect on sliding velocities relative to the control when added at the highest concentration used in the PEVK experiments (Fig. 4, *square*). There was also no binding detected between HMM and I27-PEVK-I84 using a capillary binding assay (not shown) similar to that described previously (Li et al., 1995; Kellermayer and Granzier, 1996a). We conclude that a dynamic interaction between F-actin and the PEVK domain results in a force that opposes the HMM-based motile force. This raises the possibility that a similar force arises as the thin filaments are translocated relative to titin in passively stretched sarcomeres. Such a force could make a significant contribution to the passive tension, as suggested by the passive tension decrease measured by Granzier et al. (1997) in response to selective thin filament extraction in rat cardiomyocytes.

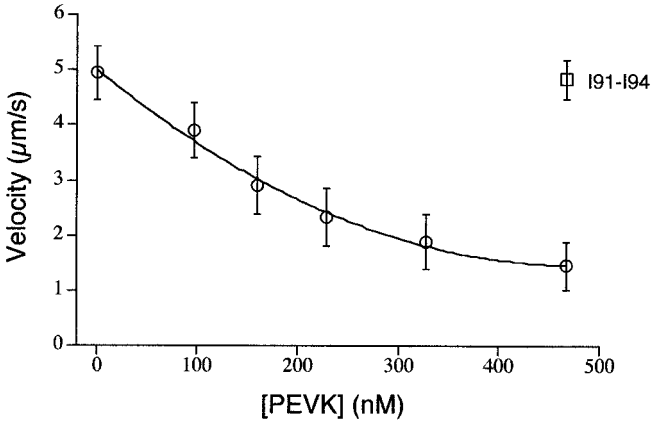

FIGURE 4 In vitro motility assay. *Circles:* F-actin sliding velocities were measured over surfaces coated with either HMM (0 nM I27-PEVK-I84) or a mixture of HMM and varying concentrations of I27-PEVK-I84 (100–475 nM). I27-PEVK-I84 inhibited velocities in a concentration-dependant manner, with a 475 nM concentration of the fragment resulting in an ~70% reduction in velocity. *Square:* A four Ig-like domain fragment (I91–I94) from titin's proximal tandem Ig segment did not effect velocities when added at the highest concentration used for I27-PEVK-I84 (475 nM). Each data point represents the mean velocity for $n = 75$ filaments. Error bars are ± SD.

PEVK–actin interaction contributes to passive tension

To probe whether PEVK–actin interaction can affect the development of passive tension, mechanical experiments with mouse cardiac myocytes were performed. The passive tension–SL relation of skinned myocytes ($n = 5$) was measured before and after incubation with I27-PEVK-I84, and again after the subsequent washout of the fragment. If the PEVK domain binds actin in the myocyte, the exogenous I27-PEVK-I84 could compete with native titin molecules for binding sites along the thin filament. The addition of the PEVK fragment therefore provides a measure of the effect of PEVK–actin interaction on passive tension generation by "competing-off" endogenous PEVK–actin interactions. Figure 5 *A* shows passive tension–SL curves for a representative cell, and Fig. 5 *B* shows the mean passive tensions versus SL for all cells (relative to control values) in the presence of the PEVK fragment (*circles*) and after washout of the fragment (*squares*). The addition of the PEVK fragment significantly decreased passive tension at all SLs, with the magnitude of the decrease inversely related to SL. The mean decrease across all SLs tested was ~20%, and ~45% of this decrease was recovered across all SL after washout of the fragment. In a recent study (C. Muhle-Goll, M. Habeck, O. Cazorla, M. Nilgos, S. Labeit, and H. Granzier, submitted for publication), incubating skinned mouse left ventricular myocytes with recombinant fragments from titin's A-band and Z-line regions had no effect on passive tension. These findings indicate that recombinant proteins do not affect passive tension nonspecifically, and suggest that the observed decrease is mediated by the actin-binding properties of I27-PEVK-I84.

S100A1 binds to the cardiac PEVK domain in vitro and in situ

S100A1 is a member of the S100 family of E-F hand calcium-binding proteins, and is the predominant S100 isoform present in the adult heart (Kato and Kimura 1985; Haimoto and Kato 1987), where it resides at high concentrations (Haimoto and Kato 1988). Because proline-rich regions, such as titin's PEVK domain often bind multiple ligands, we tested whether S100A1 can bind to the cardiac PEVK domain using an overlay technique (Kincaid et al., 1988). Binding curves (Fig. 6) were obtained in the presence (0.1 mM $CaCl_2$) and absence (1 mM EGTA) of calcium, yielding half-maximal binding values of 42.5 and 120.7 nM with and without calcium, respectively (because the binding curve determined in the presence of 1 mM EGTA is not well-saturated, the value obtained at low calcium should be considered a rough estimate). These

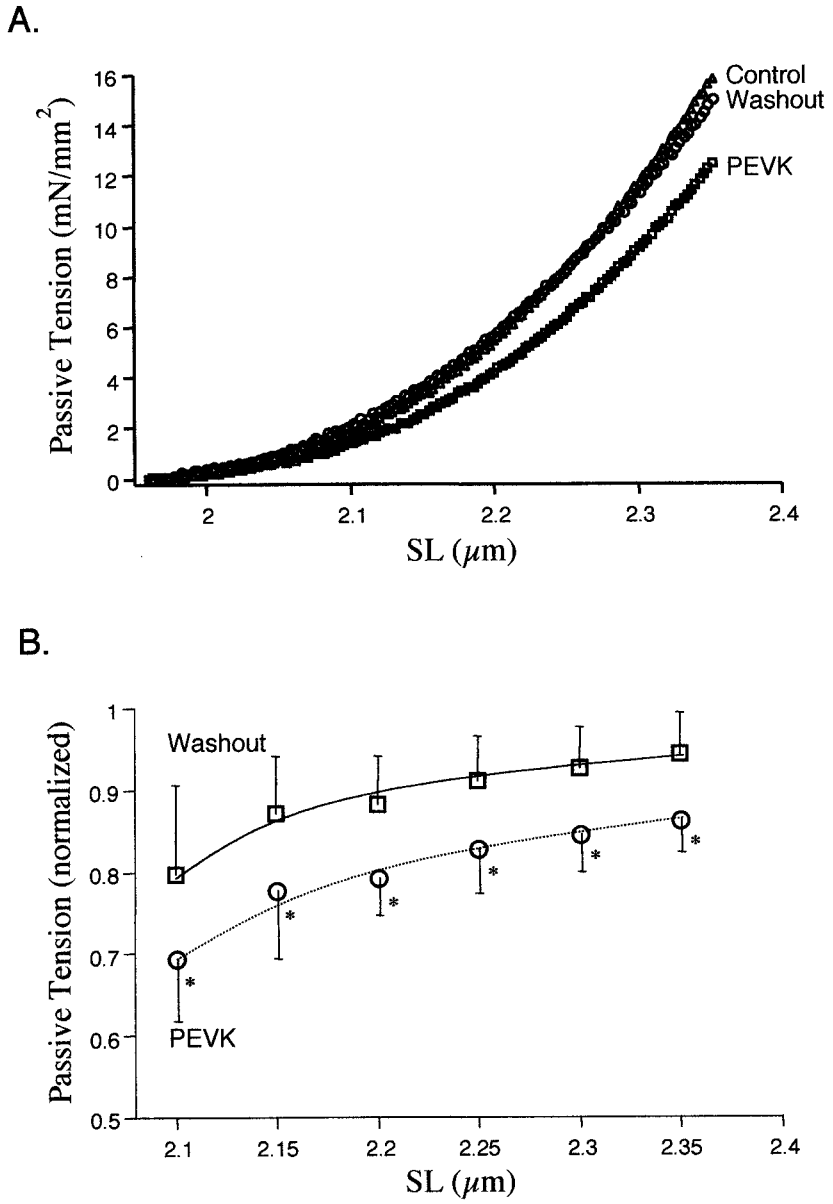

FIGURE 5 Myocyte mechanics. (*A*) Passive tension–SL curves were measured for a representative cell in relaxing solution (*triangles*), after a 40-min incubation with I27-PEVK-I84 (*squares*), and after washout of the fragment (*circles*). I27-PEVK-I84 incubation resulted in a reversible decrease in passive tension. (*B*) Mean passive tensions measured for all cells ($n = 5$) as a function of SL (normalized to the control values for each cell). I27-PEVK-I84 decreased passive tension by ~20% (*circles*) relative to the control across all SLs, with the magnitude of the decrease inversely related to SL. Across all SLs upon washout of the fragment (*squares*), ~45% of the decrease was recovered. Passive tensions in the presence of I27-PEVK-I84 were compared to both the control and washout using a Dunnet's test. Asterisks denote a significant ($p < 0.05$) difference from the control, and error bars are + (washout) or − (I27-PEVK-I84) SEM.

results indicate that S100A1 binds to the PEVK fragment in a calcium-dependent manner.

To test whether the binding observed in vitro occurs in the intact sarcomere, skinned mouse ventricular muscle strips were incubated with S100A1 in the presence of calcium, and bound proteins were detected using immuno-electron microscopy (IEM) with an antibody specific to the S100 α-subunit. Labeling varied (most likely due to variation in skinning and antibody penetration) but was typically observed at the periphery of the M-lines, and in the myofibrillar I-bands and A-bands (Fig. 7 *C*; for discussion of A-band labeling, see below). In the I-band, three labeled regions could be distinguished (Fig. 7 *C*) whose positions varied with SL (Fig. 7 *D*), suggesting that they label titin rather than the proteins of the thin filament.

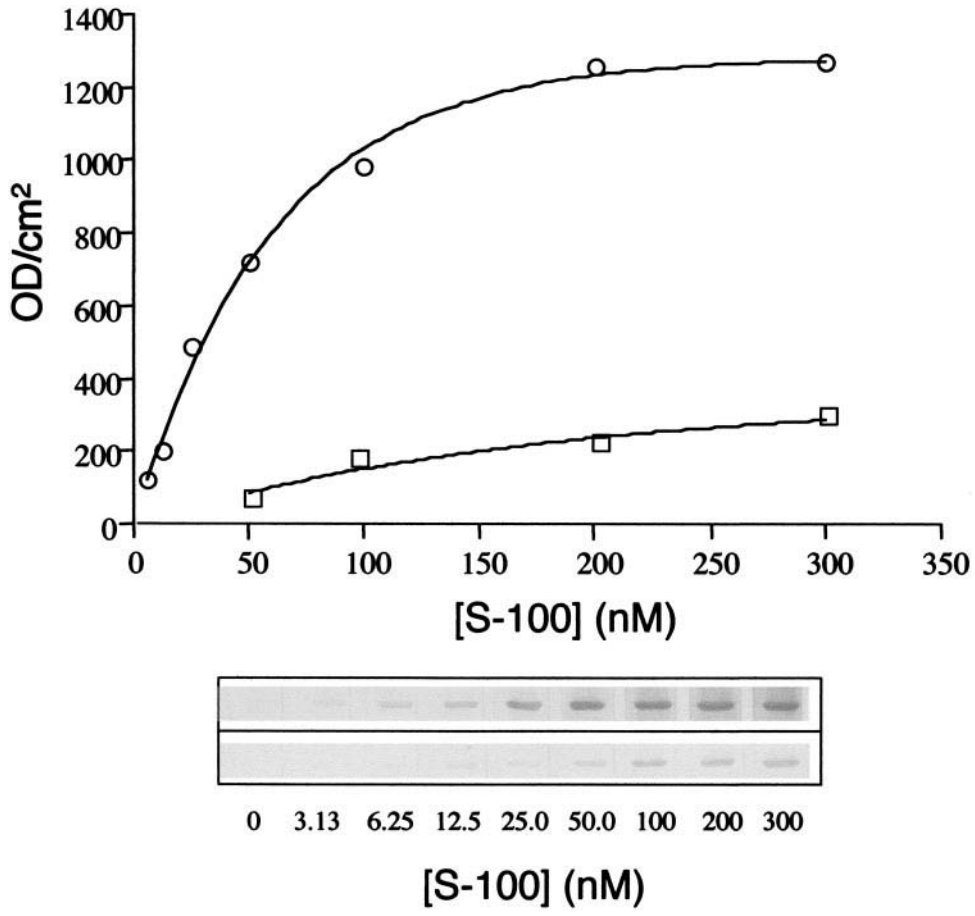

FIGURE 6 Gel overlay analysis. Biotinylated-S100A1 was allowed to bind to I27-PEVK-I84 (1 μg/lane) immobilized on a PVDF membrane, in the presence (0.1 mM $CaCl_2$) or absence (1 mM EGTA) of calcium. Bound S100 was detected with an avidin/alkaline phosphatase and a colorimetric substrate. Band intensities were determined via densitometry, and fitted with a saturable binding function, giving half-maximal binding values of ~40 nM and ~120 nM and saturation values of ~1200 OD/cm^2 and ~400 OD/cm^2 in the presence and absence of calcium, respectively.

In previous work, the extensible behaviors of the molecular subdomains comprising N2B titin's elastic region were characterized, including the PEVK domain (Trombitas et al., 1999). Sequence-specific antibodies were used to label the boundaries of each segment, and the positions of the epitopes were measured as a function of SL using IEM. Comparing the mobility of the S100 epitopes with those demarcating titin's elastic subdomains allowed us to estimate the locations of the S100 binding sites along the titin molecule. Figure 7 *D* shows the mobilities of the S100 epitopes overlaid with those of epitopes marking the boundaries of titin's various subdomains. The data reveal S100 binding within the PEVK domain, as well as within the 572-residue unique sequence of the N2B element and the C-terminal region of the proximal tandem Ig segment. The binding observed in situ is thus consistent with the in vitro results (Fig. 6), and suggests that S100A1 binds the PEVK domain of N2B titin. Interestingly, S100 also targets the unique N2B segment whose extension, along with the PEVK domain, accounts for the majority of the titin-based passive tension generated over the physiological SL range (Helmes et al., 1999; Linke et al., 1999).

S100A1 inhibits PEVK–actin interaction in a calcium-dependent manner

To determine whether S100 binding modulates the PEVK domain's actin-binding properties, a series of experiments were performed using the fluorescent surface binding assay. PEVK-coated coverslips were incubated with S100, washed, and then incubated with F-actin. Figure 8 *A* shows the relative degree of actin binding as a function of S100 concentration in the presence (0.1 mM CaC_{12}) and absence (1 mM EGTA) of calcium. There was no significant difference in actin binding at high and low levels of calcium in the absence of S100. This finding is in agreement with the co-sedimentation results that found no calcium effect on PEVK–actin binding affinity (Fig. 2 *B*). Pre-incubating the PEVK fragment with S100A1, however, inhibited binding in a concentration-dependent manner. Moreover, this inhibition was greatly enhanced by calcium. Actin–PEVK bind-

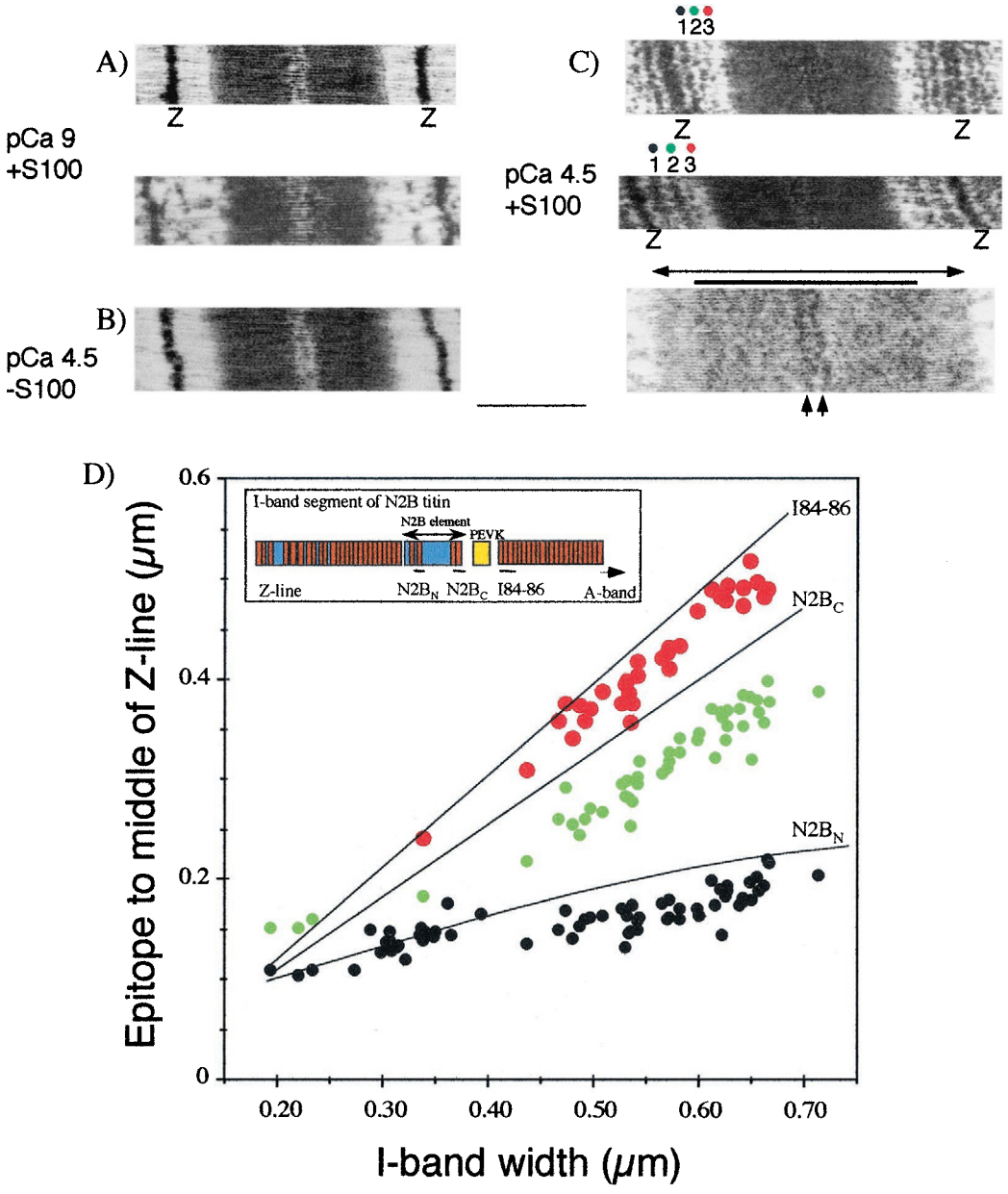

FIGURE 7 Immuno-electron microscopy. *A–C*, Electron micrographs of mouse left ventricular muscle strips. (*A*) Strips incubated with 7.5 μM S100A1 at pCa 9. The majority of sarcomeres did not contain S100 epitopes (*top*), although, occasional, sarcomeres displayed spotty labeling (*bottom*). (*B*) Control strips incubated at pCa 4.5 without S100 showed no labeling. A similar absence of labeling was seen at pCa 9 (not shown). (*C*) Strips incubated with 7.5 μM S100A1 at pCa 4.5. Several labeled regions could be distinguished in the central I-band region, each of which were mobile with respect to the Z-line at varying degrees of sarcomere stretch (*top*, *middle*). Bottom micrograph shows that labeling was also observed in the inner ~3/4 (indicated by thick line) of the A-band (*arrow bars*) in a region that includes the C-zone, as well as near the periphery of the M-line (*arrows*). The near M-line epitopes are 69 $\pm$ 0.8 nm (n = 17) apart. Calibration bar: 1 μm for all micrographs except for bottom micrograph of *C*, which is 0.5 μm. (*D*) Distances between the midpoint of the I-band labeled regions and the middle of the Z-line as a function of I-band width. Lines indicate previously determined (Trombitas et al., 1999) linear regression fits of epitopes marking the ends of the PEVK domain (I84–I86 and N2Bc) and the 572-residue unique N2B sequence (N2Bc and N2Bn). The S100 epitope mobilities are consistent with binding to the C-terminal end of the proximal tandem Ig (*red symbols*), the unique N2B sequence (*blue symbols*), and the PEVK domain (*yellow symbols*). *Inset:* Schematic of titin's I-band domain organization showing the locations of the N2Bn, N2Bc, and I84–I86 antigens.

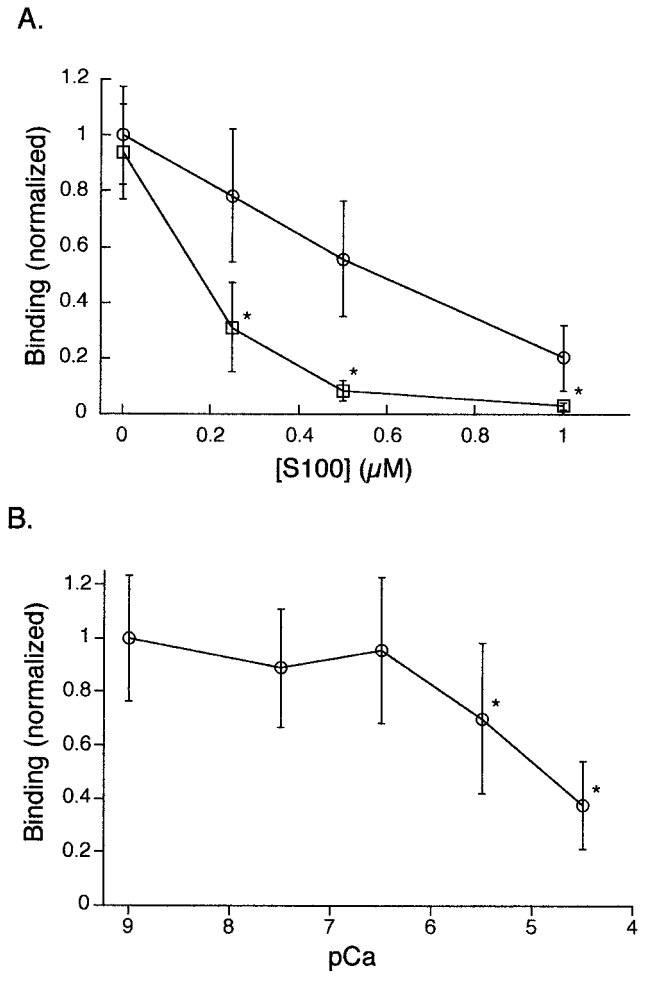

FIGURE 8 S100A1 inhibits actin-PEVK interaction. I27-PEVK-I84-coated surfaces (0.3 μM) were incubated with S100A1, washed, and then incubated with fluorescently labeled F-actin. (*A*) Actin-PEVK binding as a function of S100A1 concentration in the presence (0.1 mM $CaCl_2$; *squares*) or absence (1 mM EGTA; *circles*) of calcium. In control experiments (0 nM S100), PEVK–actin interaction was unaffected by calcium. S100A1 inhibited PEVK–actin interaction in a concentration-dependant manner, with the degree of inhibition significantly enhanced by calcium at each S100A1 concentration tested. Data points represent the mean number of filaments bound per FOV for $n = 7$ experiments, with 20 FOV/experiment. Values ± calcium were compared with a Student's *t*-test, and statistically significant ($p < 0.05$) differences are denoted with asterisks. Error bars are ± SD. (*B*) F-actin binding to PEVK-coated surfaces that were pre-incubated with a fixed concentration of S100A1 (170 nM) at a range of pCa values. Relative to the value at pCa 9, binding was significantly ($p < 0.05$) reduced at pCa values of 5.5 and 4.5. Data points represent the mean number of actin filaments bound per FOV for $n = 9$ experiments, with 20 FOV/experiment. pCa 9 values were compared to pCa 7.5–4.5 values using a Dunnet's test. Error bars are ±SD.

ing was significantly reduced at high calcium relative to that measured at low calcium for all concentrations of S100 used. At an S100:PEVK molar ratio of approximately 1:1 (340 nM S100), PEVK–actin binding was almost completely abolished (~3% of control value) in the presence of calcium. In light of our S100–PEVK binding results (Figs. 6 and 7), the observed decrease is likely due to a direct interaction between S100A1 and the PEVK fragment that prevents actin-PEVK binding.

In Fig. 8 *B*, the effect of S100 on PEVK–actin interaction was measured as a function of calcium concentration. F-actin was allowed to bind to a PEVK-coated surface that was pre-incubated with a fixed concentration of S100 at pCa levels ranging from 9 to 4.5. Relative to the value at pCa 9, actin binding was reduced by ~30% and ~60% at pCa values of 5.5 and 4.5, respectively. The pCa range in which this effect was detected is within the range where half-maximal activation occurs in intact cardiac muscle (Bers 2000), and coincides with previous work that demonstrates that S100A1 binds calcium and undergoes conformational changes within the pCa range from ~6–4 (Baudier et al., 1986). Moreover, Baudier et al. also demonstrated that the presence of free $[Mg^{2+}]$ decreases the affinity of S100A1 for calcium. Because the free $[Mg^{2+}]$ in our experiments (~1.5 mM) likely exceeds that found in the working myocyte (~0.5–1.0 mM; see e.g., Silverman et al., 1994; Freudenrich et al., 1992), the pCa range in which we detected the reduction in binding may be underestimated.

Calcium/S100A1 alleviates PEVK-based motility inhibition

In the previous motility experiments (Fig. 4) PEVK–actin interaction resulted in a force that opposed the sliding of actin filaments relative to the PEVK domain. From our binding studies (Fig. 8), one would expect the inhibition of HMM-driven motility to be alleviated in the presence of S100A1 and calcium. This hypothesis was tested by measuring the velocities of actin filaments sliding over a surface that was coated with either HMM or a mixture of HMM and the PEVK fragment, and was pre-incubated (before the addition of F-actin) with and without S100A1 in the presence of 0.1 mM $CaCl_2$. In the absence of S100, the PEVK fragment inhibited F-actin velocity by ~50% of the control value (Fig. 9, *middle* versus *top panels*). When the HMM/PEVK-coated surface was pre-incubated with S100A1, the velocity was ~150% of the value obtained without S100 (in the presence PEVK), representing a ~50% recovery of the PEVK-based inhibition (Fig. 9, *middle* versus *bottom panels*). This recovery requires S100A1, because calcium alone had no effect on F-actin velocities measured in the presence of the PEVK fragment (2.3 μm/s ± 0.6 (SD) versus 2.6 μm/s ± 0.7 (SD) in the presence and absence of calcium, respectively). This result is consistent with the in vitro binding data, which failed to detect an effect of calcium on PEVK–actin interaction (Figs. 2 *B* and 8 *A*). To exclude an HMM-mediated effect of S100, control experiments were performed in which S100A1 was added in the absence of the PEVK fragment. There was no significant difference in the mean velocity measured in these experiments (4.4 μm/s ± 0.4 (SD)) compared to that measured with HMM only

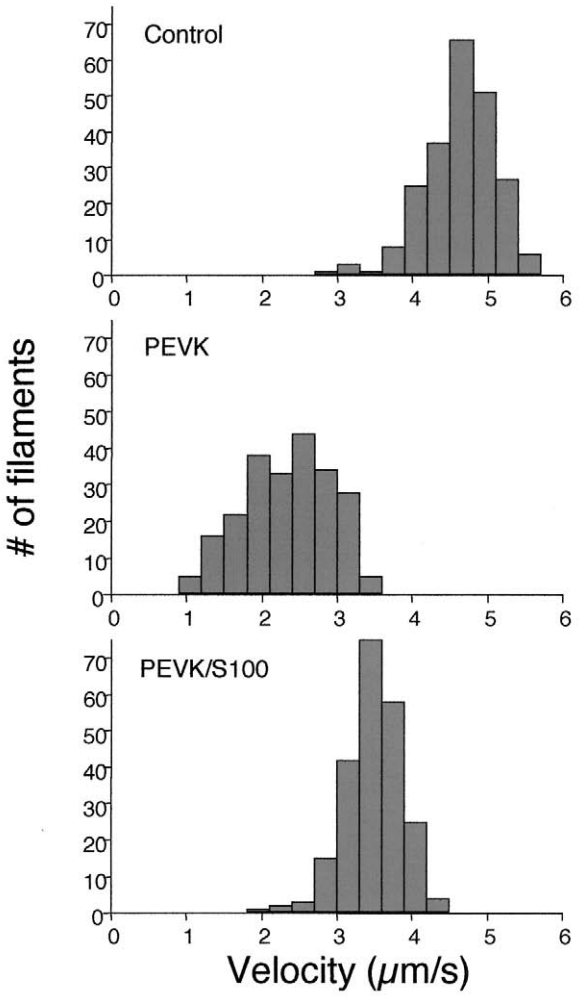

FIGURE 9 Calcium/S100A1 alleviates PEVK-based inhibition of in vitro motility. F-actin velocities were measured over surfaces coated with either HMM (*top*) or a mixture of HMM and I27-PEVK-I84 (*middle* and *bottom*) in the presence of 0.1 mM $CaCl_2$. I27-PEVK-I84 (450 nM) inhibited sliding velocities by ~50% relative to the control (2.3 ± 0.6 μm/s versus 4.6 ± 0.5 μm/s in PEVK-treated and control, respectively (±SD)). Calcium/S100A1 (3 μM) alleviated the PEVK-based motility inhibition by ~50%, to 3.5 ± 0.4 μm/s (±SD). Each histogram contains velocities pooled from $n = 3$ experiments, with 75 filaments/experiment (225 total filaments). PEVK velocities (*middle*) were determined to be significantly different from both the control (*top*) and the PEVK + S100 (*bottom*) using a Dunnet's test ($p < 0.05$).

(4.6 μm/s ± 0.5 (SD)). In summary, although calcium alone does not affect PEVK–actin interaction, calcium/S100A1 inhibits PEVK–actin interaction, and alleviates PEVK-based inhibition of in vitro motility.

DISCUSSION

We surveyed the subdomains of titin's extensible region for binding interactions with F-actin, which could potentially modulate titin's elastic properties. The existence of such interactions is suggested by previous work on rat cardiac myocytes (Granzier et al., 1997; Trombitas and Granzier 1997) in which thin filament extraction from the extensible region of titin resulted in a significant passive tension reduction at SLs >~2.0 μm. Because the tandem Ig segments are nearly straight at these SLs, the effect was unlikely to result from interaction between actin and the tandem Ig segments (Granzier et al., 1997). In agreement with this notion are the results from the present study that failed to detect binding between actin and a fragment encompassing 8 Ig repeats from the distal tandem Ig segment (Fig. 2 *A*), and the results of others (Linke et al., 1997). At SLs above ~2.0 μm, passive force is determined by extension of the PEVK segment and the N2B unique sequence (Trombitas et al., 1999). Although no binding was detected between actin and the N2B unique sequence (Fig. 2 *A*), we demonstrate that a recombinant cardiac PEVK fragment binds readily to F-actin. These results are in agreement with the recent findings of Linke and co-workers (Kulke et al., 2001), who also reported binding between the cardiac PEVK domain and F-actin. A possible explanation for an earlier study, which did not detect binding between the N2B PEVK domain and F-actin (Linke et al., 1997) may be the inherent difficulties in expressing and purifying the PEVK region of titin.

In the present study, the interaction between the PEVK domain and F-actin was characterized, and its physiological significance investigated using a multi-faceted approach, including in vitro binding assays, in vitro motility, myocyte mechanics, and immunoelectron microscopy. Our findings indicate that a dynamic interaction between the PEVK domain and F-actin makes a significant contribution to the passive tension. Evidence that PEVK–actin interaction can be regulated in a calcium-sensitive manner by the soluble calcium-binding protein S100A1 is also provided.

Mechanism underlying PEVK–actin interaction

F-actin contains a large patch of negatively charged residues on its exposed surface (Kabsch et al., 1990), and several actin-binding proteins are known to bind to this region via basic charge clusters (e.g., Friederich et al., 1992; Pfuhl et al., 1994; Fulgenzi et al., 1998). The results of our binding studies suggest that PEVK-actin interaction also includes an electrostatic component. Both the skeletal and cardiac PEVK fragments exhibited decreased binding in response to increased IS, with the skeletal PEVK exhibiting weaker binding at intermediate IS and a greatly enhanced IS sensitivity (Fig. 3 *B*). Only the cardiac N2B PEVK bound F-actin at physiological IS s. These differences in actin-binding affinity may be explained by their different charge characteristics of the cardiac and skeletal PEVK fragments, which have theoretical isoelectric points (pI) of 9.7 and 8.0, respectively. At physiological pH, the cardiac PEVK therefore carries a greater net positive charge, which likely

facilitates its interaction with the negatively charged actin filament.

Assuming that the actin-binding propensity of the PEVK domain is indeed related to its net charge, it is possible to make predictions about the binding properties of the PEVK domains expressed in different titin isoforms. The majority of the PEVK sequences in all titin isoforms are comprised of basic (pI ~ 9–10) 27–28-residue repeats, termed PPAK repeats, that are rich in proline (Greaser, 2001). In addition, the larger versions of the PEVK domain expressed in skeletal titins and the cardiac N2BA isoform contain highly acidic (pI ~ 4.0) polyglutamic acid (E) regions interspersed with the PPAK repeats (Greaser, 2001). The presence of the poly-E regions gives the larger PEVK isoforms a net acidic character. For example, the soleus muscle PEVK has a predicted pI of 5.1. In contrast, the cardiac N2B PEVK lacks poly-E segments and has a pI (9.70) that is characteristic of the PPAK repeats that comprise >75% of its primary structure. The cardiac N2B PEVK may therefore be unique among the PEVK isoforms in its ability to bind actin. However, a conclusive determination of whether the PEVK domains of skeletal muscle titins can bind actin will require future studies using constructs that include the full-length versions of the PEVK expressed in each titin isoform.

In addition to their net positive charge, the PPAK repeats are also rich in proline (~25%). Proline-rich regions (PRRs) often assume extended conformations, such as the polyproline II (PPII)-helix that was recently predicted for skeletal muscle PEVK fragments (Gutierrez-Cruz et al., 2000; Ma et al., 2001). Due to the conformational restrictions that proline residues impose on the polypeptide backbone, PRRs experience a relatively small reduction of entropy upon ligand binding (Williamson 1994). This property makes them energetically favorable sites for protein-protein interactions, and there are numerous examples of PRRs that perform binding functions in vivo (for review, see Williamson 1994). The binding of actin by the PPAK-rich N2B PEVK may therefore be both electrostatically and thermodynamically favorable.

Physiological significance of PEVK–actin interaction

As the myocardium is passively stretched during diastole, the thin filaments are translated relative to the PEVK domain. We investigated how PEVK–actin interaction might influence this process using an in vitro motility assay technique in which F-actin was propelled over a surface coated with either HMM alone or a mixture of HMM and the PEVK fragment. The addition of the PEVK fragment inhibited F-actin velocities in a concentration-dependent manner (Fig. 4). The inhibition is likely due to a tethering mechanism similar to that proposed in previous titin-related motility studies (Li et al., 1995; Kellermayer and Granzier 1996a). Because F-actin readily binds to the PEVK fragment in the fluorescent surface-binding assay (Figs. 3 and 8), a similar interaction could transiently tether the motile actin filaments to the surface of the assay chamber via surface-bound PEVK fragments. An HMM-based effect on velocity is unlikely because HMM does not bind to the PEVK fragment, and mixtures of HMM and a similar-sized fragment containing only Ig-like domains had no effect on velocity (Fig. 4). Moreover, studies have shown that actin velocities are independent of HMM surface density over a wide range of HMM concentrations (Homsher et al., 1993). The proposed mechanism of motility inhibition, in which a dynamic interaction between the PEVK domain and F-actin results in a force that opposes HMM-driven motility, is also supported by the reversibility of inhibition in the presence of calcium/S100 (see below).

To determine whether PEVK–actin interaction affects passive tension generation, mechanical experiments with mouse cardiac myocytes were conducted, in which I27-PEVK-I84 was added to skinned myocytes to compete with endogenous titin molecules for binding sites on the thin filament. The presence of I27-PEVK-I84 significantly reduced passive tension at all SLs, with a mean reduction of ~20%, whereas washout of the fragment led to a mean passive tension recovery of ~45%. Passive tension in skinned myocytes is almost entirely due to the extension of titin's I-band spanning segment (Granzier and Irving 1995), and the significant reduction of passive tension in the presence of I27-PEVK-I84 can therefore be considered a titin-based effect. Because binding was detected only in the PEVK region of titin's extensible segment (Fig. 2 *A*), we conclude that PEVK–actin interactions in the sarcomere (which are likely abolished by the addition of the PEVK fragment) make a significant contribution to the passive tension.

It is possible, however, that the exogenous PEVK fragment could also compete off other interactions in the sarcomere. For example, a segment of titin located near the Z-line is known to strongly associate with the thin filament (Linke et al., 1997; Trombitas and Granzier 1997), and this interaction could be reversibly uncoupled during I27-PEVK-I84 incubation and washout. This possibility is unlikely though, because the abolishment of titin–actin interaction near the Z-line via extensive gelsolin extraction recruits the near Z-line titin into the extensible pool, leading to an increase (rather than a decrease) in passive tension at SLs between slack and 2.2 μm (Granzier et al., 1997). It is also possible that I27-PEVK-I84 inhibits binding between the thin filament and the I111–I112 region of titin, which has been shown previously to bind F-actin (Jin, 1995). However, an effect of I111–I112–actin binding on passive tension is not consistent with the sarcomeric location of the I111–I112 region of titin, which is not extensible in mouse cardiac muscle (Trombitas et al., 2000). A potential explanation for the lack of a full recovery of passive tension upon washout of I27-PEVK-I84 could be related to a small de-

crease in passive tension that was observed in parallel control experiments in which the PEVK fragment was omitted (not shown). This decrease is likely due to "run-down" during the protocol, because we did not witness any recovery of passive tension in the control.

A mechanism by which PEVK–actin interaction could contribute to passive tension in cardiac myocytes is suggested by the motility results, which show that PEVK–actin interaction results in a force that opposes the sliding of actin relative to titin. The SL-dependence of the passive tension decrease measured in the myocyte experiments is consistent with this hypothesis, because the PEVK domain may have less lateral freedom to interact with the thin filament as it becomes fully extended at longer SLs. Binding between titin and the thin filament could also effectively shorten the length of titin's extensible region, resulting in higher fractional extensions at a given SL. As shown previously (Granzier et al., 1997; Kellermayer et al., 1997; Trombitas et al., 1998b), the fractional extensions of titin's extensible segments correlate with the magnitude of passive tension.

S100A1 as a potential regulator of PEVK–actin interaction

S100A1 resides at high concentrations in striated muscles (Kato and Kimura 1985), and has been shown to bind to the SR-ryanodine receptor (Treves et al., 1997), the actin-capping protein Cap-Z (Ivanenkov et al., 1996), nebulin (Gutierrez-Cruz et al., 2000), and the kinase domain of the titin-related protein twitchin (Heierhorst et al., 1996). Here, we show that S100A1 can bind to the N2B PEVK domain both in vitro and in situ. The in vitro results (Figs. 6 and 8) reveal that the binding of S100A1 to the PEVK domain inhibits PEVK-actin interaction in a calcium-sensitive manner. These findings, and the results of others (Zimmer 1991), suggest that F-actin does not bind to S100A1. However, in light of a recent report of S100A1 interaction with F-actin (Mandinova et al., 1998), this possibility was tested in both the co-sedimentation assay and the visual surface-binding assay (data not shown). No binding was detected between F-actin and S100A1 in either the presence (0.1 mM $CaCl_2$) or absence (1 mM EGTA) of calcium.

Previous S100A1 binding studies have deduced a consensus sequence ((K/R)(L/I)XWXXIL) for S100A1 recognition (Ivanenkov et al., 1996), and S100A1 interactions with proteins containing the consensus can be inhibited by a peptide called TRTK-12 (Garbuglia et al., 1999). Although the PEVK domain lacks this consensus sequence, there are several reports of S100A1 interactions with targets that also lack a consensus site and that are unaffected by TRTK-12 (Treves et al., 1997; Garbuglia et al., 2000). It thus appears that S100A1 can bind its target proteins via multiple mechanisms, and the sequence and structural determinants for its target recognition are not yet fully understood.

Reports of S100A1 binding to protein domains that also bind calmodulin (Baudier et al., 1987; Heierhorst et al., 1996; Treves et al., 1997) may give insights into S100A1–PEVK interaction. Calmodulin is known to bind amphiphilic helices on its target proteins (for review, see O'Neil and DeGrado 1990). PPII-helices can also have amphiphilic properties (Stapley and Creamer 1999), and a PEVK PPAK-repeat was recently determined to contain substantial PPII-helix content (Gutierrez-Cruz et al., 2000; Ma et al., 2001). Considering that PPAK repeats comprise >75% of the N2B PEVK (Greaser, 2001), and, given its abundance of charged and hydrophobic residues (~40% charged and ~22% hydrophobic), it is possible that the N2B PEVK contains PPII-helices with amphiphilic properties. Future studies aimed at defining the S100A1 binding site(s) within the PEVK domain could establish whether S100A1 does indeed bind to such regions.

Immunolabeling revealed that S100A1 binds at several locations in the I-band and A-band of mouse cardiac muscle in the presence of calcium (Fig. 7). It is unlikely that I-band binding results from interaction between S100A1 and the thin filament because the positions of the S100A1 epitopes changed with respect to the Z-line as sarcomeres were stretched (Fig. 7, *C* and *D*). Instead, the mobility of the S100 binding sites indicates binding between S100A1 and the I-band region of titin. Whether the binding partner in the A-band is also titin or another thick-filament protein remains to be established. If S100A1 does bind titin in the A-band, the location of the binding sites suggests interaction with titin's super-repeat domains (located in the C-zone of the A-band) and a region ~15-nm C-terminal of titin's kinase domain (located ~50 nm from the center of the A-band; Obermann et al., 1997). Comparing the positions of the I-band S100 binding sites as a function of SL with those of epitopes marking the various segments within titin's extensible region suggests that S100 binds to the PEVK domain, the N2B unique sequence and the C-terminal region of the proximal tandem Ig segment.

A functional role for S100A1-PEVK binding is suggested by our in vitro motility results, which show that calcium/S100A1 can alleviate the PEVK-based inhibition of F-actin motility (Fig. 9). By inhibiting PEVK–actin interaction, calcium/S100A1 may provide the sarcomere with a mechanism to free the thin filament from titin before active contraction and thereby reduce titin-based force. Considering that the cytosolic S100A1 is likely to be constant during the heart's pumping cycle, fluctuations in free calcium may result in a cyclic regulation of PEVK–actin interaction. The results of ter Keurs and co-workers, which demonstrate that the stiffness of rat cardiac trabeculae increases as calcium levels decay during the diastolic interval, are consistent with this hypothesis (Stuyvers et al., 1997a,b, 1998, 2000). Further testing of whether calcium/S100 regulates PEVK–actin interaction in the sarcomere during systole would require methods that allow the effects of S100A1 to be observed at

high calcium levels, without interference from active contraction. Although methods exist for depressing actomyosin interaction (Zhao et al., 1995; Meyer et al., 1998), they do not completely abolish active force development, and their effect on PEVK–actin interaction is unknown. Future work is therefore needed to elucidate the full functional significance of calcium/S100-based regulation of PEVK–actin interaction.

In summary, our findings show that cardiac titin's PEVK domain binds F-actin, and that this interaction is a significant contributor to the passive tension. We also show that S100A1 can bind to the PEVK domain both in vitro and in situ. S100 binding inhibits PEVK–actin interaction, and may aid in freeing the thin filament from titin before active contraction. The targeting of S100A1 to titin's primary force-generating elements (the N2B element and the PEVK domain) suggests that S100A1 may be an important regulator of titin's intrinsic elastic properties, and its interactions with other proteins.

We gratefully acknowledge financial support from the following sources: The American Heart Association, Northwest Affiliate (predoctoral fellowship to R.Y.), the Deutsche Forschungsgemeinschaft (La 668/6-1 to S.L.), the Hungarian Science Foundation (OTKA F025353 to M.S.Z.K.), and the National Institutes of Health (HL61497 and HL62881 to H.G. and HL62466 to M.G.). M.S.Z.K. is a Howard Hughes Medical Institute International Research Scholar and is a recipient of the Bolyai János Fellowship of the Hungarian Academy of Sciences. I91–I98 and I91–I94 plasmids were kindly provided by Dr. M. Gautel. Thanks to A. Yamasaki for help in performing binding assays, and to Drs. B. Slinker and C. Omoto for comments on the manuscript.

REFERENCES

Baudier, J., N. Glasser, and D. Gerard. 1986. Ions binding to S100 proteins. I. Calcium- and zinc-binding properties of bovine brain S100 alpha alpha, S100a (alpha beta), and S100b (beta beta) protein: Zn^{2+} regulates Ca^{2+} binding on S100b protein. *J. Biol. Chem.* 261:8192–8203.

Baudier, J., D. Mochly-Rosen, A. Newton, S. H. Lee, D. E. Koshland, Jr., and R. D. Cole. 1987. Comparison of S100b protein with calmodulin: interactions with melittin and microtubule-associated tau proteins and inhibition of phosphorylation of tau proteins by protein kinase C. *Biochemistry.* 26:2886–2893.

Bers, D. M. 2000. Calcium fluxes involved in control of cardiac myocyte contraction. *Circ. Res.* 87:275–281.

Bradford, M. M. 1976. A rapid and sensitive method for the quantitation of microgram quantities of protein utilizing the principle of protein–dye binding. *Anal. Biochem.* 72:248–254.

Cazorla, O., A. Freiburg, M. Helmes, T. Centner, M. McNabb, Y. Wu, K. Trombitas, S. Labeit, and H. Granzier. 2000. Differential expression of cardiac titin isoforms and modulation of cellular stiffness. *Circ. Res.* 86:59–67.

Chang, C. T., C. S. Wu, and J. T. Yang. 1978. Circular dichroic analysis of protein conformation: inclusion of the beta-turns. *Anal. Biochem.* 91:13–31.

Fabiato, A. 1988. Computer programs for calculating total from specified free or free from specified total ionic concentrations in aqueous solutions containing multiple metals and ligands. *Methods Enzymol.* 157: 378–417.

Freiburg, A., K. Trombitas, W. Hell, O. Cazorla, F. Fougerousse, T. Centner, B. Kolmerer, C. Witt, J. S. Beckmann, C. C. Gregorio, H. Granzier, and S. Labeit. 2000. Series of exon-skipping events in the elastic spring region of titin as the structural basis for myofibrillar elastic diversity. *Circ. Res.* 86:1114–1121.

Friederich, E., K. Vancompernolle, C. Huet, M. Goethals, J. Finidori, J. Vandekerckhove, and D. Louvard. 1992. An actin-binding site containing a conserved motif of charged amino acid residues is essential for the morphogenic effect of villin. *Cell.* 70:81–92.

Freudenrich, C. C., E. Murphy, S. Liu, and M. Lieberma. 1992. Magnesium homeostasis in cardiac cells. *Mol. Cell Biochem.* 114:97–103.

Fulgenzi, G., L. Graciotti, A. L. Granata, A. Corsi, P. Fucini, A. A. Noegel, H. M. Kent, and M. Stewart. 1998. Location of the binding site of the mannose-specific lectin comitin on F-actin. *J. Mol. Biol.* 284: 1255–1263.

Funatsu, T., E. Kono, H. Higuchi, S. Kimura, S. Ishiwata, T. Yoshioka, K. Maruyama, and S. Tsukita. 1993. Elastic filaments in situ in cardiac muscle: deep-etch replica analysis in combination with selective removal of actin and myosin filaments. *J. Cell Biol.* 120:711–724.

Garbuglia, M., M. Verzini, A. Hofmann, R. Huber, and R. Donato. 2000. S100A1 and S100B interactions with annexins. *Biochim. Biophys. Acta.* 1498(2–3):192–206.

Garbuglia, M., M. Verzini, R. R. Rustandi, D. Osterloh, D. J. Weber, V. Gerke, and R. Donato. 1999. Role of the C-terminal extension in the interaction of S100A1 with GFAP, tubulin, the S100A1- and S100B-inhibitory peptide, TRTK-12, and a peptide derived from p53, and the S100A1 inhibitory effect on GFAP polymerization. *Biochem. Biophys. Res. Commun.* 254:36–41.

Gordon, A. M., M. A. LaMadrid, Y. Chen, Z. Luo, and P. B. Chase. 1997. Calcium regulation of skeletal muscle thin filament motility in vitro. *Biophys. J.* 72:1295–1307.

Granzier, H., M. Helmes, and K. Trombitas. 1996. Nonuniform elasticity of titin in cardiac myocytes: a study using immunoelectron microscopy and cellular mechanics. *Biophys. J.* 70:430–442.

Granzier, H., M. Kellermayer, M. Helmes, and K. Trombitas. 1997. Titin elasticity and mechanism of passive force development in rat cardiac myocytes probed by thin-filament extraction. *Biophys. J.* 73:2043–2053.

Granzier, H. L., and T. C. Irving. 1995. Passive tension in cardiac muscle: contribution of collagen, titin, microtubules, and intermediate filaments. *Biophys. J.* 68:1027–1044.

Granzier, H. L., and K. Wang. 1993. Gel electrophoresis of giant proteins: solubilization and silver-staining of titin and nebulin from single muscle fiber segments. *Electrophoresis.* 14:56–64.

Greaser, M. L., S. Wang, M. Berri, P. E. Mozdziak, and Y. Kumazawa. 2000. Sequence and mechanical implications of cardiac PEVK. *Adv. Exp. Med. Biol.* 481:53–63.

Greaser, M. 2001. Identification of new repeating motifs in titin. *Proteins.* 43:145–149.

Gregorio, C. C., H. Granzier, H. Sorimachi, and S. Labeit. 1999. Muscle assembly: a titanic achievement? *Curr. Opin. Cell Biol.* 11:18–25.

Gutierrez-Cruz, G., A. H. Van Heerden, and K. Wang. 2000. Modular motif, structural folds and affinity profiles of PEVK segment of human fetal skeletal muscle titin. *J. Biol. Chem.* 276:7442–7449.

Haimoto, H., and K. Kato. 1987. S100a0 (alpha alpha) protein, a calcium-binding protein, is localized in the slow-twitch muscle fiber. *J. Neurochem.* 48:917–923.

Haimoto, H., and K. Kato. 1988. S100a0 (alpha alpha) protein in cardiac muscle. Isolation from human cardiac muscle and ultrastructural localization. *Eur. J. Biochem.* 171:409–415.

Heierhorst, J., B. Kobe, S. C. Feil, M. W. Parker, G. M. Benian, K. R. Weiss, and B. E. Kemp. 1996. Ca^{2+}/S100 regulation of giant protein kinases. *Nature.* 380:636–639.

Helmes, M., K. Trombitas, T. Centner, M. Kellermayer, S. Labeit, W. A. Linke, and H. Granzier. 1999. Mechanically driven contour-length adjustment in rat cardiac titin's unique N2B sequence: titin is an adjustable spring. *Circ. Res.* 84(11):1339–1352.

Homsher, E., F. Wang, and J. Sellers. 1993. Factors affecting filament velocity in in vitro motility assays and their relation to unloaded shortening velocity in muscle fibers. *Adv. Exp. Med. Biol.* 332:279–289.

Ivanenkov, V. V., R. V. Dimlich, and G. A. Jamieson, Jr. 1996. Interaction of S100a0 protein with the actin capping protein, CapZ: characterization of a putative S100a0 binding site in CapZ alpha- subunit. *Biochem. Biophys. Res. Commun.* 221:46–50.

Jin, J. P. 1995. Cloned rat cardiac titin class I and class II motifs. Expression, purification, characterization, and interaction with F-actin. *J. Biol. Chem.* 270:6908–6916.

Kabsch, W., H. G. Mannherz, D. Suck, E. F. Pai, and K. C. Holmes. 1990. Atomic structure of the actin:DNase I complex. *Nature.* 347:37–44.

Kato, K., and S. Kimura. 1985. S100ao (alpha alpha) protein is mainly located in the heart and striated muscles. *Biochim. Biophys. Acta.* 842: 146–150.

Kellermayer, M. S., and H. L. Granzier. 1996a. Calcium-dependent inhibition of in vitro thin-filament motility by native titin. *FEBS Lett.* 380:281–286.

Kellermayer, M. S., and H. L. Granzier. 1996b. Elastic properties of single titin molecules made visible through fluorescent F-actin binding. *Biochem. Biophys. Res. Commun.* 221:491–497.

Kellermayer, M. S., S. B. Smith, H. L. Granzier, and C. Bustamante. 1997. Folding–unfolding transitions in single titin molecules characterized with laser tweezers. *Science.* 276:1112–1116.

Kimura, S., K. Maruyama, and Y. P. Huang. 1984. Interactions of muscle beta-connectin with myosin, actin, and actomyosin at low ionic strengths. *J. Biochem. (Tokyo).* 96:499–506.

Kincaid, R. L., M. L. Billingsley, and M. Vaughan. 1988. Preparation of fluorescent, cross-linking, and biotinylated calmodulin derivatives and their use in studies of calmodulin-activated phosphodiesterase and protein phosphatase. *Methods Enzymol.* 159:605–626.

Kron, S. J., Y. Y. Toyoshima, T. Q. Uyeda, and J. A. Spudich. 1991. Assays for actin sliding movement over myosin-coated surfaces. *Methods Enzymol.* 196:399–416.

Kulke, M., S. Fujita-Becker, D. Manstein, M. Gautel, and W. A. Linke. 2001. PEVK-titin inhibits actin filament sliding in the in-vitro motility assay. *Biophys. J.* 80:495 [Abstract].

Labeit, S., and B. Kolmerer. 1995. Titins: giant proteins in charge of muscle ultrastructure and elasticity. *Science.* 270:293–296.

Labeit, S., B. Kolmerer, and W. A. Linke. 1997. The giant protein titin. Emerging roles in physiology and pathophysiology. *Circ. Res.* 80: 290–294.

Laemmli, U. K. 1970. Cleavage of structural proteins during the assembly of the head of bacteriophage T4. *Nature.* 227:680–685.

Li, Q., J. P. Jin, and H. L. Granzier. 1995. The effect of genetically expressed cardiac titin fragments on in vitro actin motility. *Biophys. J.* 69:1508–1518.

Linke, W. A., M. Ivemeyer, S. Labeit, H. Hinssen, J. C. Ruegg, and M. Gautel. 1997. Actin–titin interaction in cardiac myofibrils: probing a physiological role. *Biophys. J.* 73:905–919.

Linke, W. A., M. Ivemeyer, P. Mundel, M. R. Stockmeier, and B. Kolmerer. 1998a. Nature of PEVK-titin elasticity in skeletal muscle. *Proc. Natl. Acad. Sci. U.S.A.* 95:8052–8057.

Linke, W. A., D. E. Rudy, T. Centner, M. Gautel, C. Witt, S. Labeit, and C. C. Gregorio. 1999. I-band titin in cardiac muscle is a three-element molecular spring and is critical for maintaining thin filament structure. *J. Cell Biol.* 146:631–644.

Linke, W. A., M. R. Stockmeier, M. Ivemeyer, H. Hosser, and P. Mundel. 1998b. Characterizing titin's I-band Ig domain region as an entropic spring. *J. Cell Sci.* 111:1567–1574.

Ma, K., L. Kan, and K. Wang. 2001. Polyproline ii helix is a key structural motif of the elastic PEVK segment of titin. *Biochemistry.* 40:3427–3438.

Mandinova, A., D. Atar, B. W. Schafer, M. Spiess, U. Aebi, and C. W. Heizmann. 1998. Distinct subcellular localization of calcium binding S100 proteins in human smooth muscle cells and their relocation in response to rises in intracellular calcium. *J. Cell Sci.* 111:2043–2054.

Margossian, S. S., and S. Lowey. 1982. Preparation of myosin and its subfragments from rabbit skeletal muscle. *Methods Enzymol.* 85:55–71.

Maughan, D. W., and R. E. Godt. 1989. Equilibrium distribution of ions in a muscle fiber. *Biophys. J.* 56:717–722.

Meyer, M., B. Keweloh, K. Guth, J. W. Holmes, B. Pieske, S. E. Lehnart, H. Just, and G. Hasenfuss. 1998. Frequency-dependence of myocardial energetics in failing human myocardium as quantified by a new method for the measurement of oxygen consumption in muscle strip preparations. *J. Mol. Cell Cardiol.* 30:1459–1470.

O'Neil, K. T., and W. F. DeGrado. 1990. How calmodulin binds its targets: sequence independent recognition of amphiphilic alpha-helices. *Trends Biochem. Sci.* 15:59–64.

Obermann, W. M., Gautel, M., Weber, K., Furst, D. O. 1997. Molecular structure of the sarcomeric M band: mapping of titin and myosin binding domains in myomesin and the identification of a potential regulatory phosphorylation site in myomesin. *EMBO J.* 16:211–220.

Pardee, J. D., and J. A. Spudich. 1982. Purification of muscle actin. *Methods Enzymol.* 85:164–181.

Pfuhl, M., S. J. Winder, and A. Pastore. 1994. Nebulin, a helical actin binding protein. *EMBO J.* 13:1782–1789.

Politou, A. S., M. Gautel, M. Pfuhl, S. Labeit, and A. Pastore. 1994. Immunoglobulin-type domains of titin: same fold, different stability? *Biochemistry.* 33:4730–4737.

Politou, A. S., D. J. Thomas, and A. Pastore. 1995. The folding and stability of titin immunoglobulin-like modules, with implications for the mechanism of elasticity. *Biophys. J.* 69:2601–2610.

Silverman, H. S., F. Di Lisa, R. C. Hui, H. Miyata, S. J. Sollott, R. G. Hanford, E. G. Laketta, and M. D. Stern. 1994. Regulation of intracellular free Mg^{2+} and contraction in single adult mammalian cardiac myocytes. *Am. J. Physiol. Cell Physiol.* 266:C222–C233.

Stapley, B. J., and T. P. Creamer. 1999. A survey of left-handed polyproline II helices. *Protein Sci.* 8:587–595.

Stuyvers, B. D., M. Miura, J. P. Jin, and H. E. ter Keurs. 1998. Ca(2+)-dependence of diastolic properties of cardiac sarcomeres: involvement of titin. *Prog. Biophys. Mol. Biol.* 69:425–443.

Stuyvers, B. D., M. Miura, and H. E. ter Keurs. 1997a. Diastolic viscoelastic properties of rat cardiac muscle; involvement of Ca^{2+}. *Adv. Exp. Med. Biol.* 430:13–28.

Stuyvers, B. D., M. Miura, and H. E. ter Keurs. 1997b. Dynamics of viscoelastic properties of rat cardiac sarcomeres during the diastolic interval: involvement of Ca^{2+}. *J. Physiol.* 502:661–677.

Stuyvers, B. D., M. Miura, and H. E. ter Keurs. 2000. Ca(2+)-dependence of passive properties of cardiac sarcomeres. *Adv. Exp. Med. Biol.* 481: 353–366.

Treves, S., E. Scutari, M. Robert, S. Groh, M. Ottolia, G. Prestipino, M. Ronjat, and F. Zorzato. 1997. Interaction of S100A1 with the Ca^{2+} release channel (ryanodine receptor) of skeletal muscle. *Biochemistry.* 36:11496–11503.

Trinick, J., and L. Tskhovrebova. 1999. Titin: a molecular control freak. *Trends Cell Biol.* 9:377–380.

Trombitas, K., A. Freiburg, T. Centner, S. Labeit, and H. Granzier. 1999. Molecular dissection of N2B cardiac titin's extensibility. *Biophys. J.* 77:3189–3196.

Trombitas, K., and H. Granzier. 1997. Actin removal from cardiac myocytes shows that near Z line titin attaches to actin while under tension. *Am J. Physiol. Cell Physiol.* 273:C662–C670.

Trombitas, K., A. Rodkan, A. Freiburg, T. Centner, Y. Wu, S. Labeit, H. Granzier. 2000. Extensibility of isoforms of cardiac titin: variation in fractional extension provides a basis for diastolic stiffness diversity. *Biophys. J.* 79:3226–3234.

Trombitas, K., M. Greaser, S. Labeit, J. P. Jin, M. Kellermayer, M. Helmes, and H. Granzier. 1998b. Titin extensibility in situ: entropic elasticity of permanently folded and permanently unfolded molecular segments. *J. Cell Biol.* 140:853–859.

Wang, K. 1996. Titin/connectin and nebulin: giant protein rulers of muscle structure and function. *Adv. Biophys.* 33:123–134.

Wang, S. M., and M. L. Greaser. 1985. Immunocytochemical studies using a monoclonal antibody to bovine cardiac titin on intact and extracted myofibrils. *J. Muscle Res. Cell Motil.* 6:293–312.

Williamson, M. P. 1994. The structure and function of proline-rich regions in proteins. *Biochem. J.* 297:249–260.

Witt, C. C., N. Olivieri, T. Centner, B. Kolmerer, S. Millevoi, J. Morell, D. Labeit, S. Labeit, H. Jockusch, and A. Pastore. 1998. A survey of the primary structure and the interspecies conservation of I-band titin's elastic elements in vertebrates. *J. Struct. Biol.* 122:206–215.

Wolska, B. M., and R. J. Solaro. 1996. Method for isolation of adult mouse cardiac myocytes for studies of contraction and microfluorimetry. *Am J. Physiol. Heart Circ. Physiol.* 271:H1250–H1255.

Wu, Y., O. Cazorla, D. Labeit, S. Labeit, and H. Granzier. 2000. Changes in titin and collagen underlie diastolic stiffness diversity of cardiac muscle. *J. Mol. Cell Cardiol.* 32:2151–2162.

Zahn, R., C. von Schroetter, and K. Wuthrich. 1997. Human prion proteins expressed in *Escherichia coli* and purified by high-affinity column refolding. *FEBS Lett.* 417:400–404.

Zhao, L., N. Naber, and R. Cooke. 1995. Muscle cross-bridges bound to actin are disordered in the presence of 2,3-butanedione monoxime. *Biophys. J.* 68:1980–1990.

Zimmer, D. B. 1991. Examination of the calcium-modulated protein S100 alpha and its target proteins in adult and developing skeletal muscle. *Cell Motil. Cytoskel.* 20:325–337.